ELSEVIER

Journal of Molecular Catalysis A: Chemical 118 (1997) 301–309

JOURNAL OF MOLECULAR CATALYSIS A: CHEMICAL

Catalytic transformation of cyclohexanol over aluminophosphate-based molecular sieves

S.P. Elangovan [a], V. Murugesan [b,*]

[a] *Department of Chemistry, Sri Venkateswara College of Engineering, Sriperumbudur – 602 105, India*
[b] *Department of Chemistry, Anna University, Madras – 600 025, India*

Received 29 February 1996; accepted 5 September 1996

Abstract

Catalytic transformation of cyclohexanol over $AlPO_4$-5, $AlPO_4$-11, SAPO-5, SAPO-11, VAPO-5, VAPO-11, CoAPO-5, CoAPO-11, NAPO-5, NAPO-11, ZAPO-5 and ZAPO-11 has been studied. The main product formed from this transformation is cyclohexene. The product distribution is influenced by acidity, inverse weight hourly space velocity $(WHSV)^{-1}$ and temperature. Increase of $(WHSV)^{-1}$ and temperature increase the formation of dehydrogenated product with simultaneous decrease of dehydrated product. The effect of various parameters like acidity, $(WHSV)^{-1}$ and temperature on the conversion of cyclohexanol and the product distribution has been fully discussed.

Keywords: Aluminophosphate; Molecular sieves; Cyclohexanol; Cyclohexene; Cyclohexanone

1. Introduction

Catalytic conversion of cyclohexanol has been often used as model reaction to evaluate the acidity and catalytic activity of catalysts [1]. The decomposition of cyclohexanol gives mainly either cyclohexene or cyclohexanone. It has been reported that the quantity of cyclohexene formation depends on the presence of Bronsted acid sites [2]. However, the formation of cyclohexanone from cyclohexanol by dehydrogenation is gaining importance in view of its industrial applications. Cyclohexanone is used in the manufacture of adipic acid and caprolactum which are the main raw materials for the production of nylon-6,6 and nylon-6 respectively. Aluminophosphate-based molecular sieves are gaining importance due to the presence of a variety of acid sites and acidic strengths [3,4] and this can also be evaluated from the transformation of cyclohexanol. The present study has been undertaken to report the catalytic transformation of cyclohexanol over unsubstituted and substituted (Si, V, Co, Ni and Zn) $AlPO_4$-5 and $AlPO_4$-11, and the effects of acidity, $(WHSV)^{-1}$ and temperature on the conversion of cyclohexanol and product distribution.

2. Experimental

2.1. Synthesis and characterization

$AlPO_4$-5, $AlPO_4$-11 and silicon, vanadium, cobalt, nickel and zinc containing $AlPO_4$-5 and

* Corresponding author. Fax: +91-44-2352870.

PII S1381-1169(96)00391-3

$AlPO_4$-11 were synthesized by the methods described already [5–10]. Experimental conditions employed in the synthesis of these molecular sieves are presented in Table 1.

X-ray diffraction analysis was carried out employing a Siemens D500 diffractometer in the scan range 2θ between 5 and 50° using Cu Kα as source. The peaks were identified with reference to compilation of simulated XRD powder pattern [11]. Unit cell parameters were calculated using a standard least square refinement technique. IR spectra of the samples were recorded in a Bruker IFS 66v FT-IR spectrophotometer whereas ESR analysis was carried out using a variant E 112 spectrophotometer at room temperature. TGA of the samples were carried out with a Mettler TA 3000 system at a scanning rate of 20°C/min in a stream of dry air. Inductively coupled plasma (ICP) ARL 3410 with a minitorch was used to find the chemical composition of the samples. Acidity was measured by temperature programmed desorption (TPD) of pyridine using TGA (Mettler TA 3000 system). Prior to adsorption, the samples were evacuated to 10^{-3} Torr at 450°C for 2 to 3 h. Then pyridine in a closed vessel was allowed to equilibrate at room temperature. TG analysis was carried out up to 500°C at a scanning rate of 10°C/min. From the weight loss at different temperature ranges, acidity and acidic strength in mmol/g were determined.

Surface area measurements were carried out in a Micromeritics Pulse Chemisorb 2700 using nitrogen as adsorbent at −176°C. Initially the samples were degasified at 200°C for 2 h in a flow of oxygen.

2.2. Catalytic studies

The reactor system was a fixed-bed, vertical, downward-flow type reactor made up of a quartz tube of 40 cm length and 2 cm internal diameter. The quartz reactor was heated to the requisite temperature with the help of a tubular furnace controlled by a digital temperature controller cum indicator. The bottom of the reactor was provided with a thermowell in which a chromel–alumel thermocouple was kept to measure the temperature at the middle of the catalyst bed. About 2 g of the catalyst (20–40 mesh size) were placed in the reactor and supported on either side with a thin layer of quartz wool and ceramic beads. The top portion of the reactor was connected to a glass bulb having two inlets. Reactant was fed into the reactor through

Table 1
Conditions employed for the synthesis of aluminophosphate-based molecular sieves [a]

Structure	Gel composition	pH		Temp. (°C)
		Before synthesis	After synthesis	
$AlPO_4$-5	$1TEA:1Al_2O_3:1P_2O_5:40H_2O$	4.5	9.4	175
$AlPO_4$-11	$1DPA:1Al_2O_3:1P_2O_5:40H_2O$	4.5	10.1	200
SAPO-5	$0.1SiO_2:1TEA:1Al_2O_3:1P_2O_5:40H_2O$	4.9	9.8	175
SAPO-11	$0.1SiO_2:1DPA:1Al_2O_3:1P_2O_5:40H_2O$	3.9	8.5	200
VAPO-5	$0.1V_2O_5:1TEA:1Al_2O_3:1P_2O_5:40H_2O$	4.2	9.6	175
VAPO-11	$0.1V_2O_5:1DPA:1Al_2O_3:1P_2O_5:40H_2O$	3.2	9.7	200
CoAPO-5	$0.1CoO:1TEA:1Al_2O_3:1P_2O_5:40H_2O$	4.2	9.3	175
CoAPO-11	$0.1CoO:1DPA:1Al_2O_3:1P_2O_5:40H_2O$	3.8	9.4	200
NAPO-5	$0.1NiO:1TEA:1Al_2O_3:1P_2O_5:40H_2O$	4.9	9.0	175
NAPO-11	$0.1NiO:1DPA:1Al_2O_3:1P_2O_5:40H_2O$	4.0	9.1	200
ZAPO-5	$0.1ZnO:1TEA:1Al_2O_3:1P_2O_5:40H_2O$	4.4	9.5	175
ZAPO-11	$0.1ZnO:1DPA:1Al_2O_3:1P_2O_5:40H_2O$	3.9	9.7	200

[a] Crystallization time = 22 h.

one inlet by a syringe infusion pump that can be operated at different flow rates. The bottom of the reactor was connected to a coiled condenser and a receiver in which the products were collected.

The liquid products collected for the first 15 minutes of each run were discarded and analysis was made only of the products collected after this time. This was done to ensure that steady state had been attained in the reaction over the catalyst and also to allow for any temperature fluctuation near the start of the reaction. After each catalytic run, the catalyst was regenerated by passing air free from carbon dioxide through the reactor at 500°C for 6 h. In the case of cobalt and vanadium-substituted samples during the regeneration, V^{4+} is oxidized to V^{5+} and Co^{2+} to Co^{3+}. Hence, these two types of catalyst were reduced to their original oxidation states by passing pure hydrogen over them for a period of 1 h at the reaction temperature before the catalytic run. The liquid products were analyzed using a Hewlett-Packard gas chromatograph 5890 Å with a flame ionization detector. Carbowax column and nitrogen as carrier gas were used. The injector, detector and oven temperatures for the cyclohexanol transformation were 180, 225 and 140–220°C, respectively.

3. Results and discussion

3.1. Characterization

3.1.1. X-ray diffraction (XRD)

X-ray powder patterns of as synthesized $AlPO_4$-5 and $AlPO_4$-11 are shown in Fig. 1 as representative figure. The patterns are well matched with reported patterns [11]. The stability of structure after successful removal of templates has also been confirmed from XRD after calcination of the samples. Unit cell parameters and unit cell volume for both as-synthesized and calcined samples are presented in Table 2. The unit cell volumes of $AlPO_4$-5 and $AlPO_4$-11 are smaller than the corresponding substituted aluminophosphate molecular sieves. Increased unit

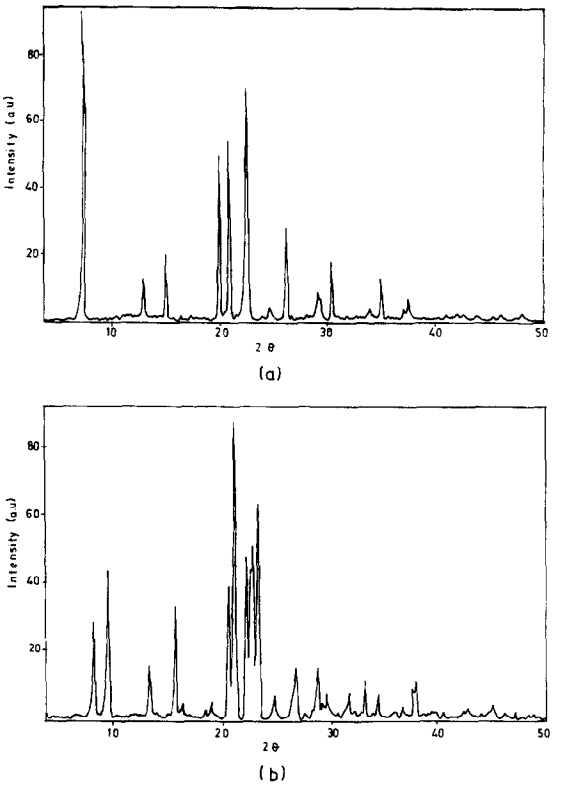

Fig. 1. X-ray diffraction pattern of (a) $AlPO_4$-5, (b) $AlPO_4$-11.

cell volume in the case of substituted aluminophosphate molecular sieves is a convincing evidence for the isomorphous substitution of M^{n+} in the aluminophosphate framework. However, the decrease in unit cell volume for

Table 2
Unit cell parameters and unit cell volume of as-synthesized and calcined aluminophosphate-based molecular sieves

Sample	As-synthesized				Calcined			
	a (Å)	b (Å)	c (Å)	V (Å^3)	a (Å)	b (Å)	c (Å)	V (Å^3)
$AlPO_4$-5	13.64	13.64	8.49	1368	13.64	13.64	8.37	1349
$AlPO_4$-11	13.48	18.55	8.39	2099	13.45	18.56	8.31	2074
SAPO-5	13.74	13.74	8.47	1386	13.68	13.68	8.42	1365
SAPO-11	13.30	18.81	8.44	2112	13.38	18.64	8.35	2083
VAPO-5	13.69	13.69	8.62	1399	13.66	13.66	8.51	1375
VAPO-11	13.40	18.63	8.45	2109	13.63	18.24	8.39	2086
CoAPO-5	13.74	13.74	8.44	1380	13.67	13.67	8.39	1358
CoAPO-11	13.37	18.91	8.43	2131	13.71	18.73	8.13	2088
NAPO-5	13.74	13.74	8.47	1385	13.67	13.67	8.48	1372
NAPO-11	13.50	18.62	8.43	2114	13.71	18.55	8.21	2088
ZAPO-5	13.83	13.83	8.48	1404	13.78	13.78	8.42	1385
ZAPO-11	13.46	18.71	8.40	2115	13.69	18.72	8.23	2109

all the calcined samples may be attributed to the removal of strain after the loss of templates from the voids [5–8].

3.1.2. FT-IR and ESR spectra

The framework vibrations and –OH vibration from FT-IR spectra of all the samples are presented in Table 3. Noticeably the spectral features of all -5 and -11 structures are similar except that there is a variation in the –OH vibration. The –OH vibration in the substituted aluminophosphate molecular sieves is shifted to a higher wave number in comparison to the corresponding unsubstituted molecular sieves and this may be attributed to the presence of Bronsted acid sites [12].

Table 4 represents the ESR parameters of VAPO-5, VAPO-11, NAPO-5 and NAPO-11. The calculated parameters for VAPO-5 and VAPO-11 are very similar to those obtained by Montes et al. [13] and Rigutto and van Bekkum [14] showing well resolved hyperfine resonance indicating that vanadium is highly dispersed. The peaks confirm the paramagnetic species of ^{51}V with $I = 7/2$. The incorporation of nickel into the aluminophosphate framework may be evident from the data shown in Table 4 which exhibits two transitions confirming the presence of nickel. A single resonance is observed at g value of 2.03 and 2.05 for CoAPO-5 and CoAPO-11 respectively. The values are consistent with tetrahedral environment of cobalt in the framework. However, no hyperfine structure is observed and the lack of hyperfine structure, ^{59}Co with $I = 7/2$, may be due to strong spin–spin interaction between cobalt neighbors [15].

Table 3
IR spectral data of aluminophosphate-based molecular sieves

Sample	Wave number (cm^{-1})	
	Framework vibrations	–OH vibration
$AlPO_4$-5	1121, 740, 634, 558, 469	3398
$AlPO_4$-11	1112, 715, 626, 546, 468	3406
SAPO-5	1088, 737, 629, 559, 463	3603
SAPO-11	1108, 712, 627, 546, 468	3485
VAPO-5	1124, 702, 631, 558, 469	3510
VAPO-11	1124, 710, 627, 551, 471	3463
CoAPO-5	1118, 701, 630, 553, 468	3565
CoAPO-11	1123, 710, 625, 543, 466	3512
NAPO-5	1124, 732, 651, 536, 471	3412
NAPO-11	1119, 740, 638, 557, 478	3408
ZAPO-5	1121, 739, 633, 557, 469	3501
ZAPO-11	1120, 713, 643, 549, 468	3465

Table 4
ESR parameters of VAPO-5, VAPO-11, NAPO-5 and NAPO-11

Sample	$g_{\parallel}$	$g_{\perp}$	$A_{\parallel}$ (G)	$A_{\perp}$ (G)
VAPO-5	1.937	1.991	185	74
VAPO-11	1.941	1.987	189	75
NAPO-5	2.09	2.07	36	27
NAPO-11	2.08	2.07	35	25

3.1.3. Thermogravimetric analysis (TGA) and chemical analysis

TG and their corresponding derivative curves (DTG) of the samples are shown in Figs. 2 and 3. All the samples show a low temperature weight loss around 100°C which is attributed to the loss of water and high temperature weight losses in the temperature range 250–550°C may be ascribed to the desorption of templates present in the intracrystalline pores. The desorption of templates proceeds in multiple stages for substituted aluminophosphate molecular sieves. This may be possibly the release of template first as free amine at a low temperature and then by degradation of proton or metal complexed amine at high temperature [16]. The total weight loss is about 12.5, 9.9, 12.8, 12.6, 13.2, 9.8, 11.9, 8.2, 13.7, 9.5, 10.7 and 10.1% for $AlPO_4$-5, $AlPO_4$-11, SAPO-5, SAPO-11, VAPO-5, VAPO-11, CoAPO-5, CoAPO-11, NAPO-5, NAPO-11, ZAPO-5 and ZAPO-11 respectively.

The results of chemical analysis of the samples presented in Table 5 clearly indicate that silicon and vanadium substitute phosphorus in the framework whereas cobalt, nickel and zinc replace aluminium. The extent of substitution is maximum for cobalt followed by silicon, zinc and vanadium and substitution is minimum for nickel.

3.1.4. Surface area

Table 5 also shows the BET surface area of the catalysts. Nitrogen adsorption at −176°C indicates that the catalysts have surface area between 196 and 260 m^2/g. The surface area of substituted aluminophosphate molecular sieves are almost similar to the corresponding unsubstituted aluminophosphate molecular sieves. This demonstrates that the incorporation of foreign elements is not blocking the pores of the structure [16].

3.1.5. Acidity

Acidity of the catalysts was determined by TPD from pyridine desorption using TGA. The values are given in Table 6. Peaks at different temperature ranges, 136–190°C, 190–280°C and 280–390°C are considered as weak, moderate and strong acid sites respectively [17]. The observed weight loss in the temperature range, 40–136°C is due to the loss of physisorbed pyridine [12]. It is clear from the data shown in the Table 6 that $AlPO_4$-5 and $AlPO_4$-11 possess low acidity values because of the strict alternation of P–O and Al–O tetrahedra. The framework is found to be neutral in both cases and have no strong acid sites. Weak acidity was reported for $AlPO_4$-5 structure resulting in low catalytic activity [18]. The source of weak acid sites is probably due to lattice imperfections and it was suggested earlier that only an excess Al–O tetrahedra might lead to strong acid sites

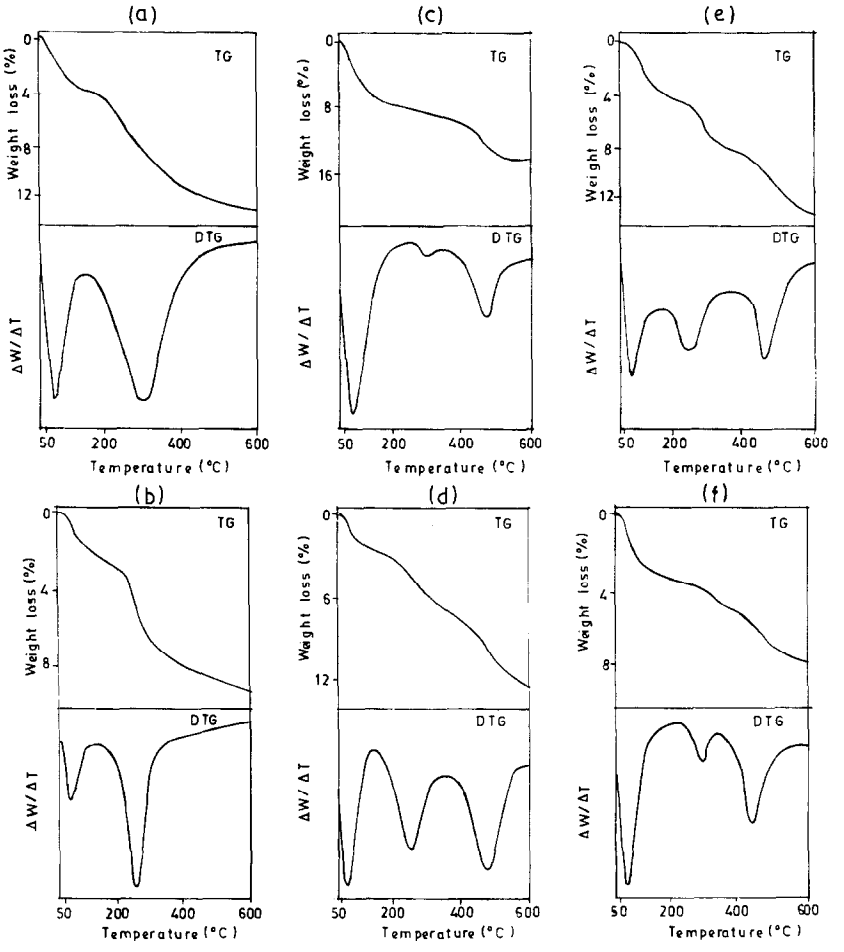

Fig. 2. TG and DTG curves of (a) $AlPO_4$-5, (b) $AlPO_4$-11, (c) SAPO-5, (d) SAPO-11, (e) VAPO-5, (f) VAPO-11.

and this requires Al–O–Al connections which is rather improbable. However, the incorporation of silicon, cobalt, zinc, vanadium and nickel may cause negative charge on the framework and this negative charge is balanced by protons or metal cations resulting in strong and moderate acid sites in the substituted aluminophosphate molecular sieves. Among the substituted aluminophosphate molecular sieves, silicon substituted molecular sieves exhibit a higher total acidity. The reason for this high value may be due to increased silicon substitution for phosphorus in the aluminophosphate framework [19] and this has been confirmed further from chemical analysis studies (Table 5). In the case of CoAPO-5 and ZAPO-5 the strong acid sites are increased considerably due to the fact that cobalt and zinc substitute for aluminium is higher than for other substituted aluminophosphate molecular sieves. SAPO-5, VAPO-5, CoAPO-5, CoAPO-11, ZAPO-5 and ZAPO-11 possess all the three types of acid sites, whereas SAPO-11, VAPO-11, NAPO-5 and NAPO-11 have only weak and moderate acid sites. $AlPO_4$-5 and $AlPO_4$-11 possess only weak acid sites, as evident in Table 6.

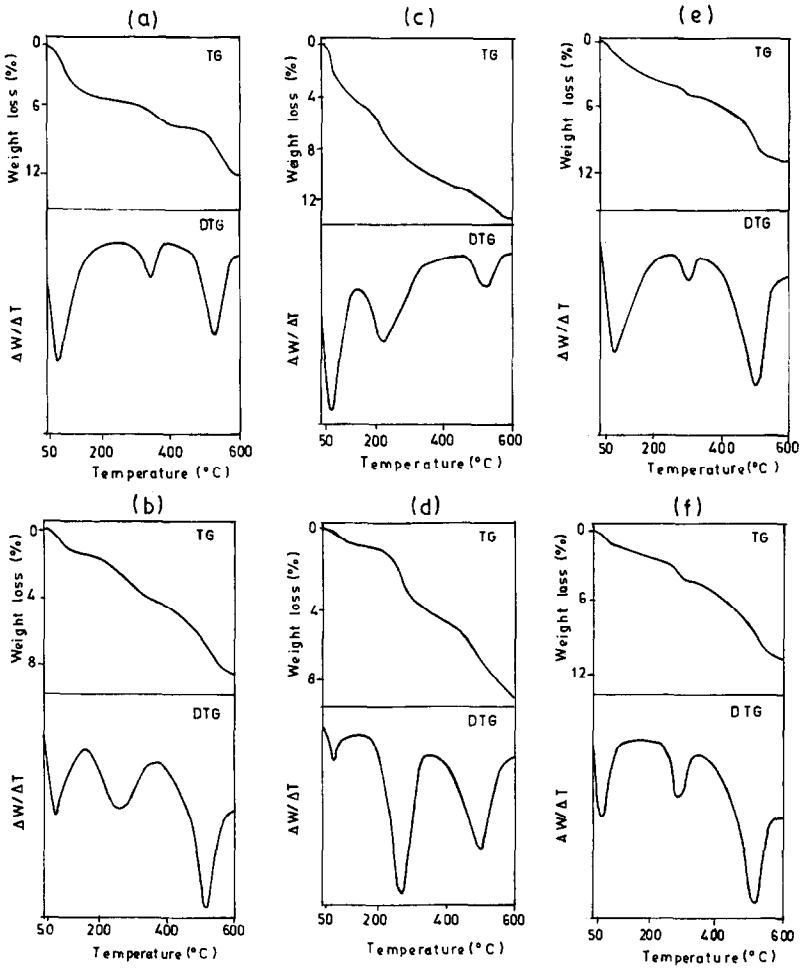

Fig. 3. TG and DTG curves of (a) CoAPO-5, (b) CoAPO-11, (c) NAPO-5, (d) NAPO-11, (e) ZAPO-5, (f) ZAPO-11.

Table 5
Chemical analysis and surface area of aluminophosphate-based molecular sieves

Sample	Molar composition	BET surface area (m^2/g)
$AlPO_4$-5	$1Al_2O_3:1P_2O_5$	221
$AlPO_4$-11	$1Al_2O_3:1P_2O_5$	204
SAPO-5	$0.08SiO_2:1Al_2O_3:0.93P_2O_5$	239
SAPO-11	$0.06SiO_2:1Al_2O_3:0.94P_2O_5$	233
VAPO-5	$0.06VO_2:1Al_2O_3:0.95P_2O_5$	226
VAPO-11	$0.06VO_2:0.99Al_2O_3:0.95P_2O_5$	206
CoAPO-5	$0.09CoO:0.91Al_2O_3:1P_2O_5$	252
CoAPO-11	$0.08CoO:0.93Al_2O_3:1P_2O_5$	196
NAPO-5	$0.05NiO:0.96Al_2O_3:0.99P_2O_5$	233
NAPO-11	$0.04NiO:0.97Al_2O_3:1P_2O_5$	199
ZAPO-5	$0.07ZnO:0.96Al_2O_3:1P_2O_5$	260
ZAPO-11	$0.06ZnO:0.95Al_2O_3:1P_2O_5$	202

Table 6
Acidity and acidic strength of aluminophosphate-based molecular sieves

Catalyst	Acidity (mmol/g)			
	Weak	Moderate	Strong	Total
$AlPO_4$-5	0.11	—	—	0.11
$AlPO_4$-11	0.08	—	—	0.08
SAPO-5	0.17	0.20	0.05	0.42
SAPO-11	0.14	0.18	—	0.32
VAPO-5	0.16	0.17	0.04	0.37
VAPO-11	0.17	0.15	—	0.32
CoAPO-5	0.14	0.16	0.08	0.38
CoAPO-11	0.11	0.14	0.05	0.30
NAPO-5	0.16	0.14	—	0.30
NAPO-11	0.14	0.12	—	0.26
ZAPO-5	0.18	0.15	0.06	0.39
ZAPO-11	0.17	0.14	0.03	0.34

3.2. Cyclohexanol transformation

The catalytic transformation of cyclohexanol over aluminophosphate-based molecular sieves gives mainly cyclohexene with small amounts of cyclohexanone, benzene and phenol. This reaction was chosen as a model reaction to evaluate the catalytic activity of aluminophosphate-based molecular sieves.

3.2.1. Effect of acidity

Table 7 presents the cyclohexanol conversion and product yield over all the catalysts at $(WHSV)^{-1}$ 1.1 h and 350°C. Cyclohexanol conversion is maximum over SAPO-5 (92.7%) and minimum over $AlPO_4$-11 (38.9%) which is in accordance with acidity values reported in Table 6. The various products formed from this transformation are cyclohexene, cyclohexanone, benzene and phenol along with small amounts of high molecular weight products. Among these, cyclohexene is the main product formed due to the presence of Bronsted acidity in the aluminophosphate-based molecular sieves. Considerable amount of cyclohexanol conversion and cyclohexene formation are found over $AlPO_4$-5 and $AlPO_4$-11 which may be attributed to the presence of terminal –OH group causing Bronsted acidity. Cobalt, zinc and nickel oxides are

Table 7
Cyclohexanol conversion and product yield over aluminophosphate-based molecular sieves [a]

Catalyst	Cyclohexanol conversion (wt%)	Product yield (wt%)				
		Cyclohexene	Cyclohexanone	Benzene	Phenol	Others
$AlPO_4$-5	46.2	43.1	2.6	—	—	—
$AlPO_4$-11	38.9	37.3	1.0	—	—	—
SAPO-5	92.7	82.1	3.1	—	—	7.2
SAPO-11	78.3	75.4	2.8	—	—	—
VAPO-5	83.6	64.2	6.9	2.3	2.6	4.8
VAPO-11	77.5	68.2	3.6	1.9	1.7	—
CoAPO-5	85.3	56.8	10.7	6.3	4.2	6.4
CoAPO-11	72.8	53.9	11.3	3.7	3.1	—
NAPO-5	70.4	51.7	8.3	4.1	2.4	2.5
NAPO-11	63.7	47.2	9.2	3.8	2.7	—
ZAPO-5	87.8	56.6	12.7	5.6	4.9	6.4
ZAPO-11	79.5	56.5	13.8	6.3	2.7	—

[a] $(WHSV)^{-1}$ = 1.1 h; Time on stream = 1 h; Temperature = 350°C.

Table 8
Effect of $(WHSV)^{-1}$ and temperature on conversion and product yield

Catalyst	Temp. (°C)	$(WHSV)^{-1}$ (h)	Conversion of cyclohexanol (wt%)	Product yield (wt%)				
				Cyclohexene	Cyclohexanone	Benzene	Phenol	Higher molecular wt product
ZAPO-5	350	0.9	82.7	59.2	11.8	4.2	2.3	4.8
		1.1	87.8	56.6	12.7	5.6	4.9	6.4
		1.3	90.7	51.7	12.9	8.9	7.2	6.5
		1.5	92.6	48.3	12.6	9.8	12.9	8.3
	300	1.1	70.8	66.8	2.8	1.2	—	—
	350	1.1	87.8	56.6	12.7	5.6	4.9	6.4
	400	1.1	94.7	49.4	21.3	8.3	6.9	7.3
	450	1.1	98.6	45.3	25.7	10.4	8.2	9.1

well known for the dehydrogenation activity and hence these metal oxides incorporated into aluminophosphate framework should give more of dehydrogenated products. But, contrary to our expectations, it gives more of dehydrated product. It may be possible that the total acidity plays dominant role in suppressing the dehydrogenation activity in the aluminophosphate catalysts. Small amount of high molecular weight products are also formed along with other products over all substituted -5 structures whereas they are not formed over -11 structures. This may be attributed to the smaller pore size of -11 structure which is not sufficient for the formation of high molecular weight products.

3.2.2. Effect of $(WHSV)^{-1}$ and temperature

Effect of $(WHSV)^{-1}$ and temperature on cyclohexanol conversion and product distribution over ZAPO-5 at 350°C is presented in Table 8. It is clear from the data shown in the table that increase of both $(WHSV)^{-1}$ from 0.9 to 1.5 h and temperature from 300 to 450°C increase the conversion of cyclohexanol. However, there is a difference in the product distribution. The main product is cyclohexene which decreases with increase in $(WHSV)^{-1}$ while the formation of benzene increases. This indicates that the cyclohexene initially formed might have undergone ring dehydrogenation to give benzene with increase of $(WHSV)^{-1}$. The increase of temperature increases the yield of cyclohexanone with simultaneous decrease in cyclohexene formation. This indicates that at higher temperature the Bronsted acid sites, which causes the formation of cyclohexene, are eliminated as water. Hence, this results more of dehydrogenated product.

4. Conclusion

Characterization of the aluminophosphate-based molecular sieves using sophisticated instruments evidenced the isomorphous substitution of Si, V, Co, Ni and Zn in the framework, structure stability, purity of the phase, acidity, chemical composition and surface area. In order to understand the nature of acid sites and product distribution under different conditions viz., temperature, and $(WHSV)^{-1}$, the catalytic transformation of cyclohexanol was carried out as a model reaction over these catalysts. It was found that increase of temperature decreases the concentration of Bronsted acid sites and consequently changes the product distribution. The isomorphous substitution of cobalt, nickel and zinc in the framework should result in dehydrogenated product, cyclohexanone. But, contrary to our expectations, these catalysts give more of dehydrated product, cyclohexene. It is envisaged that the total acidity plays dominant role in

suppressing the dehydrogenation activity in the aluminophosphate-based molecular sieves.

References

[1] M. Morita, E. Kawashima and K. Nomura, Kanazawa Daigaku, 5 (1990) 839.

[2] C.P. Bezouhanova and M.A. Al-Zihari, Catal. Lett. 11 (1991) 245.

[3] E.M. Flanigen, B.M. Lok and R.L. Patton, Pure and Appl Chem. 58 (1986) 1351.

[4] E.M. Flanigen, R.L. Patton and S.T. Wilson, Stud. Surf. Sci. Catal. 37 (1988) 13.

[5] S.P. Elangovan, V. Krishnasamy and V. Murugesan, React. Kinet. Catal Lett. 55 (1995) 153.

[6] S.P. Elangovan, V. Krishnasamy and V. Murugesan, Indian J. Chem. 34A (1995) 469.

[7] S.P. Elangovan, V. Krishnasamy and V. Murugesan, Hungarian J. Ind. Chem. 23 (1995) 119.

[8] S.P. Elangovan, V. Krishnasamy and V. Murugesan, Bull Chern. Soc. Jpn. 68 (1995) 3659.

[9] S.P. Elangovan, V. Krishnasamy and V. Murugesan, Catal. Lett. 36 (1996) 271.

[10] S.P. Elangovan, Banumathi Arabindoo, V. Krishnasamy and V. Murugesan, J. Chem. Soc. Faraday Trans. 91 (1995) 4471.

[11] R.V. Ballmoos and J.B. Higgins, Collection of Simulated X-Ray Powder Pattern of Zeolites (Butterworth, London, 1990).

[12] C.H. Halik, J.A. Lercher and H. Mayer, J. Chem. Soc. Faraday Trans. 1 84 (1988) 4457.

[13] C. Montes, M.E. Davis, B. Murray and M. Narayana, J. Phys. Chem. 94 (1990) 6431.

[14] M.S. Rigutto and H. van Bekkum, J. Mol. Catal. 81 (1993) 77.

[15] C. Montes, M.E. Davis, B. Murray and M. Narayana, J. Phys. Chem. 94 (1990) 6425.

[16] Y. Xu, P.J. Maddox and J.M. Thomas, Polyhedron 8 (1989) 819.

[17] J. Meusinger, H. Vinek and J.A. Lercher, J. Mol. Catal. 87 (1994) 263.

[18] G. Dworezkow, G. Rumplmayr, H. Mayer and J.A. Lercher, Stud. Surf. Sci. Catal. 21 (1985) 163.

[19] K.J. Chao and L.J. Leu, Stud. Surf. Sci. Catal. 49 (1989) 19.